Real time monitoring of the through thickness moisture profile of thin sheets using NMR

Jean-Christophe Perrin, Carina Waldner, Julie Bossu, Aninda Chatterjee, Ulrich Hirn

Chemical Engineering Science 251 (2022) 117464

Contents lists available at ScienceDirect

Chemical Engineering Science

journal homepage: www.elsevier.com/locate/ces

Real time monitoring of the through thickness moisture profile of thin sheets using NMR

Jean-Christophe Perrin [a,c], Carina Waldner [b,c], Julie Bossu [d,b], Aninda Chatterjee [a,c], Ulrich Hirn [b,c,*]

[a] Université de Lorraine, CNRS, LEMTA, F-54000 Nancy, France
[b] Institute of Biobased Products and Paper Technology, Graz University of Technology, Graz, Austria
[c] CD Laboratory for Fiber Swelling and Paper Performance, Inffeldgasse 23, 8010 Graz, Austria
[d] Wood Sciences Laboratory, UMR ECOFOG, Kourou, French Guiana

HIGHLIGHTS

- Analysis of *z*-directional distribution of liquids in thin, porous media over time.
- 1D NMR profiling method with high spatial and temporal resolution.
- Saturated reference enables evaluation of local liquid saturation and liquid amount.
- Time-dependent changes in liquid distribution and drying kinetics were observed.

ARTICLE INFO

Article history:
Received 1 October 2021
Received in revised form 14 January 2022
Accepted 21 January 2022
Available online 29 January 2022

Keywords:
NMR
Porous sheet
Dynamic moisture distribution
Mass transfer

ABSTRACT

The through-thickness distribution of liquids and liquid migration over time in thin, porous media is highly relevant for the production and product properties of materials such as textiles, membranes, paper, barrier materials, and thin films. We present a 1D NMR profiling method for the analysis of through-thickness liquid distribution during liquid absorption, migration, and drying of thin sheets. The good temporal resolution (1.3 s) and high spatial resolution (10 μm) make it possible to study changes of liquid distribution in sheets of about 100 μm thickness. A key aspect of our method is the simultaneous scanning of a liquid saturated reference sheet. Using a reference, local liquid saturation and absolute amount of liquid present over time can be evaluated. We studied the drying of water-based inkjet ink on paper substrates with differing water absorption behaviors. Differences in *z*-directional liquid distribution, penetration depth, and drying kinetics over time could be observed.

1. Introduction

The *z*-directional distribution of liquids in thin porous media and liquid migration over time is of interest in many fields such as textiles (Bencsik et al., 2008; Varga et al., 2009; Weder et al., 2006), membranes (Klein et al., 2013), production and printing of paper (Batchelor et al., 2004; Harding et al., 2001; Katugampola et al., 2006; Keränen et al., 2009; Tåg et al., 2010b), and barrier materials, coatings, and thin films (Bennett et al., 2003; Ciampi and McDonald, 2003; Erich et al., 2006, 2005; Hughes et al., 1996; Voogt et al., 2018; Wallin et al., 2000). Temporal changes in moisture distribution are relevant when studying processes like liquid absorption, migration, diffusion, and drying. These substrate-liquid interactions are important both in the production of thin porous media as well as for the resulting product properties.

On the production side, knowing the moisture profile in thickness direction can help to get a better understanding of the drying process and its kinetics. Time resolved moisture profiles in thickness direction can be used to distinguish different stages during a drying process (e.g. stages in which evaporation is limited by the evaporation from the surface or by the mass transport from the substrate's core to the surface (Tåg et al., 2010a)). Furthermore, temporally and spatially resolved moisture profiles enable the determination of mass transport coefficients that are needed for modelling. For example, the diffusion coefficient can be determined with the help of experimentally measured moisture profiles (Ketelaars et al., 1995). Beyond that, spatiotemporally resolved moisture profiles enable to optimize the product for its purpose. For instance, for barrier materials and water-repellant fabrics it is relevant how liquid is absorbed and distributed throughout the

* Corresponding author.
E-mail address: ulrich.hirn@tugraz.at (U. Hirn).

https://doi.org/10.1016/j.ces.2022.117464
0009-2509/

thickness of the material as it will define the material's barrier properties (compare e.g. (Bencsik et al., 2008)). Furthermore, the moisture distribution in the thickness direction during production can also have a significant impact on the final product. For example, in the production and printing of paper, the *z*-directional moisture profile during drying has a strong influence on the out-of-plane material deformation observed as paper curl (Uesaka, 2002).

In-situ monitoring of the moisture distribution in the thickness direction of thin sheets therefore is highly useful for the modeling, analysis and optimization of process unit operations for these materials. As liquid absorption, migration, diffusion and drying processes in thin porous media are fast and substrate thickness is in the range of tens of micrometers to a few millimeters, a spatially and temporally resolved method for measuring moisture distribution with both high temporal and spatial resolutions is required.

In this work we are introducing a nuclear magnetic resonance (NMR) based method for observation of the moisture profile over the thickness of thin sheets. The method uses a custom-built surface NMR coil integrated in a device that allows the uniform application of a controlled quantity of liquid to the surface of the sheet. We start with a review of the experimental methods that have been used in the literature for the measurement of moisture profiles before presenting our approach, followed by an application study observing the drying of inkjet ink on different papers.

1.1. Temporally and spatially resolved methods for measuring moisture content

There is a number of methods available which could potentially be used to determine moisture content profiles in thin sheets. They include near-infrared (NIR) spectroscopy, optical transparency, terahertz radiation, radiography methods, methods based on impedance measurements, and NMR based methods. NIR methods have been applied to study the moisture distribution in paper in thickness direction during different drying processes (Keränen et al., 2009; Tåg et al., 2010a, 2010b). However, no true spatially resolved through-thickness moisture profiles could be obtained. Instead, the moisture difference between top and bottom part of a thin sheet has been measured.

The correlation of optical transparency of porous materials and moisture content also offers the possibility for a spatiotemporally resolved moisture measurement. Such methods have also been used to study the drying of paper (Forughi et al., 2019, 2016). Although offering good spatial and temporal resolutions, this method is mainly applicable to measure lateral moisture profiles and cannot be easily adopted to determine moisture profiles in thickness direction. To capture moisture profiles in thickness direction using optical reflectance, the measurement has to be performed several times at different *z*-positions. This is only possible, if the sample is split or layers are removed (e.g. by grinding (Gane and Koivunen, 2010; Koivunen and Gane, 2012a, 2012b)), which results in a poor time and spatial resolution for *z*-directional measurements. The same is true for spatiotemporally resolved moisture content measurements with terahertz waves (compare (Banerjee et al., 2008; Kajihara et al., 2017)).

Radiography methods are based on the attenuation of radiation passing through a substance. Either gamma rays, X-rays, or neutrons can be used. Radiography methods have been used to determine moisture profiles in construction materials (e.g. (Nizovtsev et al., 2008; Pel et al., 1993)), but have also been applied to measure moisture distributions across thickness direction in textiles (Varga et al., 2009; Weder et al., 2006). The main drawback of radiography methods probably is that they are costly and not widely available.

Furthermore, also the correlation between impedance and moisture content can be used to determine moisture content profiles of paper in the *z*-direction (Batchelor et al., 2004; Katugampola et al., 2006). However, in order to measure the impedance and determine moisture content distributions in *z*-direction, electrodes have to be buried within the sample. Thus, impedance methods can be used for multilayered substrates, but are not able to give information about the *z*-directional moisture distribution in a single layer.

NMR based methods are used frequently as they are non-destructive and can be applied to a variety of samples, including paper. Leisen et al. (2002) for example used an NMR based method to study the through-plane diffusion of water in paper. Harding et al. (2001) applied NMR imaging to measuring *z*-directional moisture profiles during the drying of liquid packaging board. NMR has also been used to study the drying behavior of thin films and coatings (Bennett et al., 2003; Ciampi and McDonald, 2003; Erich et al., 2006, 2005; Hughes et al., 1996; Salamanca et al., 2001; Voogt et al., 2018; Wallin et al., 2000). The *z*-directional moisture profiles are recorded in most of these studies.

In Table 1, methods which deliver true moisture profiles in thickness direction are compared. The temporal resolution achieved in the NMR studies is highly variable, ranging from a few seconds to several tens of minutes. In the majority of the cases, the temporal resolution is dictated by the characteristic time of the phenomenon to be studied. The imaging method and hardware used must also be adapted to the system. In the case of coatings and films, the STRAFI (Hughes et al., 1996; Rosenkilde and Glover, 2002) and GARField (Bennett et al., 2003; Ciampi and McDonald, 2003; Erich et al., 2006, 2005; Hellgren et al., 2001; Voogt et al., 2018; Wallin et al., 2000) methods provide an excellent spatial resolution (up to 5 μm) thanks to an intense static magnetic field gradient. Thus, profiles through samples with thicknesses comparable to paper sheets (100 μm) can be recorded. In the case of the studies cited here, however, the temporal resolution is often limited by the low proton content of the sample and the small volume surveyed, which requires a lot of accumulation. The studies reported on paper or cellulose have been performed using more standard methods of spin echo imaging, either one-dimensional (Harding et al., 2001) or two-dimensional (Leisen et al., 2002) or TurboSpin Echo (Harding et al., 2001). In samples such as thin sheets of paper, spatial and temporal resolutions are limited by signal to noise considerations and by the extreme rapidity of the involved liquid migration process. In a recent work, NMR was used to study liquid penetration in paper with a GARField method. A high time resolution was achieved by lowering T_1 times through the addition of $CuSO_4$ to the liquids (Nicasy et al., 2021). The main drawback of this approach is that the liquid cannot be used in its original composition, and it is not clear if the addition of $CuSO_4$ influences the liquid-substrate interaction.

In the present work we detail a method with good temporal- and spatial resolution in the thickness direction – 1.3 s per moisture profile and 10 μm spatial resolution respectively – and apply this method to the drying of water-based ink on thin sheets of paper.

Our method is not innovative by the NMR imaging sequence used. Its main advantage is the combination of scanning speed and a high *z*-directional resolution of 10 μm. A full *z*-directional moisture profile is scanned within 1.3 s which makes the method particularly suited to study liquid penetration and drying kinetics in thin sheets. The good sensitivity of our method is ensured thanks to a surface coil, which has the same geometry as the studied samples (essentially 2D). The filling factor of the coil (roughly equal to the ratio sample volume/probe volume) is therefore maximized and the achievable acquisition time can be reduced. Fast in-situ studies of liquid migration and drying are furthermore enabled by integrating the liquid application into the NMR instrument. Finally, during each measurement always a *z*-directional intensity

Table 1
Comparison of methods used to measure *z*-directional moisture profiles in thin substrates.

Measurement method	Spatial resolution	Temporal resolution	Thickness of used substrate	Substrate type	Source
Gamma ray radiography	5 mm	~ 1 min	100 mm	concrete	(Nizovtsev et al., 2008)
Neutron radiography	0.5 mm	8 s	30 mm	brick	(Pel et al., 1993)
Neutron radiography	200 μm	53 s	4–6 cm	fibre fleece	(Varga et al., 2009)
X-ray tomography	20 μm	2 min	~5 mm	textiles	(Weder et al., 2006)
NMR	15 μm	4 min	3 layers, 80 μm each	3-layer-textile	(Bencsik et al., 2008)
NMR	8.7 μm	75 s/8.5 min	0.5 mm wood, 100 μm glass	alkyd coating on cover glass; wood glued to glass	(Bennett et al., 2003)
NMR	17 μm	1 min	300–1280 μm	PVOH films	(Ciampi and McDonald, 2003)
NMR	0.5 μm	10 min	100–200 μm	alkyd coating on cover glass	(Erich et al., 2005)
NMR	3.3 μm	10 min	~250 μm	alkyd coating on cover glass	(Erich et al., 2006)
NMR	15.6 μm	24 s	559 μm	liquid packaging board	(Harding et al., 2001)
NMR	8.74 μm	10 min	200–400 μm	latex and alkyd films	(Hellgren et al., 2001)
NMR	100 μm	1–2 h	1–2 mm	sodium silicate film	(Hughes et al., 1996)
NMR	0.05 mm	17 min/60 min	1.2 mm	paper	(Leisen et al., 2002)
NMR	1.3 mm	5 min	20 mm	wood ash	(MacMillan et al., 2002)
NMR	195 μm	13 s	10–18 mm	glass fiber bundles	(Neacsu et al., 2007)
NMR	14.5 μm	10 ms	90–165 μm	nylon membranes, printing paper	(Nicasy et al., 2021)
NMR	0.39 mm	30 min	4 mm	pulp	(Nilsson et al., 1996)
NMR	20 μm	5 min	20 mm but measured only at top 300 μm	sap wood	(Rosenkilde and Glover, 2002)
NMR	40.6 μm and 18.75 μm	8.5 min	60–1200 μm	thick film of waterborne colloidal particles	(Salamanca et al., 2001)
NMR	14 μm	2 to 3 min	400 μm	latex films	(Voogt et al., 2018)
NMR	9 μm	5 min	200–300 μm	latex films	(Wallin et al., 2000)
NMR	**10 μm**	**1.3 s**	**100 μm**	**paper**	**this work**

profile of a fully liquid saturated sheet is simultaneously measured as a reference, which permits calculation of the liquid saturation profile across the sheet during drying.

2. Materials and methods

2.1. 1D-NMR profiling

The NMR experiments were performed on a Bruker BioSpec 24/40 spectrometer operating at the proton Larmor frequency of 100.36 MHz. The system was equipped with a 6 cm ID magnetic field gradient system (BGAs) producing a maximum intensity of 1 T/m.

The NMR probe was a custom-built 1.8 cm diameter single turn copper strip loop printed on CuFlon® (Polyflon Company). This coil was used for both radiofrequency emission and NMR signal reception. More details about its design are given in a previous publication (Klein et al., 2013).

The measuring cell has been specially developed to be able to apply a thin layer of liquid on the surface of a strip of paper directly inside the NMR spectrometer and only a fraction of a second before beginning the measurement (Fig. 1). The cell is composed of PVC plates, with nylon clamping screws. The liquid container was cut out of the neck of a mineral water bottle, in direct contact with a 25 mm wide marker tip (Molotow™, Germany). The paper strip is pulled from outside the spectrometer: it first passes under the marker tip which acts as an application sponge, and then reaches the NMR probe immediately after application. The strip is then stopped and the 1D moisture profiles are recorded as a function of time.

The 1D NMR imaging sequence is depicted in Fig. 2. A pair of radiofrequency (r.f.) pulses $\{\pi/2, \pi\}$ separated in time by $TE/2$ produces a "spin echo" NMR signal at time TE. During the acquisition of the signal, a magnetic field gradient of amplitude g is turned ON for spatial encoding. The 1D profile is obtained by Fourier transform of the temporal signal. The echo time (TE) was set to 6.8 ms and the repetition time (TR) to 155 ms. $N = 8$ scans were accumulated to increase the signal-to-noise ratio, giving a time resolution between consecutive 1D liquid concentration profiles of 1.24 s. Each profile contains 256 points in a field of view of 2.5 mm, corresponding to a nominal spatial resolution of 9.77 μm/-point. The sensitive surface of the coil is about 2.5 cm^2, so that the sample volume probed by each point of the profile is about 0.79 mm^3.

The MRI acquisition of moisture profiles through a thin layer of a few tens of micrometers must be done with care because the direction of the magnetic field gradient g must be strictly orthogonal to the plane of the layer. To do this, we adjusted the imaging direction by finely combining the three orthogonal components provided by the gradient coil system. Misalignments of only a few tenths of a degree affect the shape of the profiles, which become rounded and wider than the nominal thickness of the sample (compare (Klein et al., 2013)). In order to measure profiles as square as possible, we used an ink saturated reference sheet, placed between the NMR coil and the study sample (Fig. 1d). The two sheets being parallel to each other, the initial alignment of the reference sheet guarantees the correct positioning of the study sheet after impregnation. We also note that paper curl due to the presence of water can introduce distortions in the moisture profile. This phenomenon can be reduced to a minimum by holding the paper strip between the two PVC plates but cannot be avoided completely. The reference layer is also used to evaluate the amount of water in the profiles. Since the MRI acquisition sequence used is weighted by both T_1 and T_2 NMR relaxation times of the water protons in the paper fibers (Harding et al., 2001), the intensities measured in the saturated reference sheet provides the reference values by which the measurements are normalized. The relaxation times were measured at a frequency of 20 MHz on a benchtop spectrometer (Bruker Minispec MQ20) at 25 °C. In the saturated samples considered, $T_1 \sim 250$ ms and $T_2 \sim 40$ ms, with a variation

b)

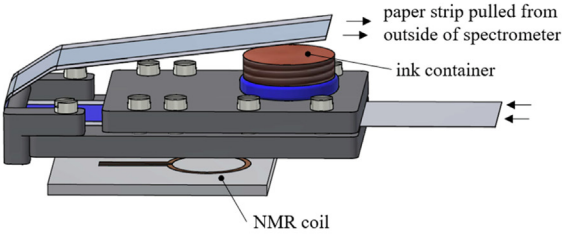

c)

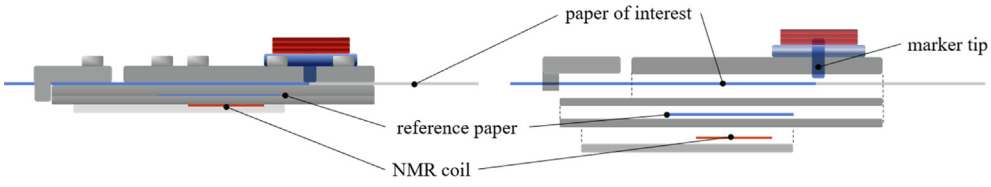

d)

Fig. 1. a) Front view of the NMR spectrometer with a 33 mm-wide paper strip installed before the start of a series of experiments. b) Photograph of the experimental setup outside the spectrometer. c) Schematic representation of the measuring cell and the NMR coil. d) Exploded view, showing the location of the reference paper between the NMR coil and the paper of interest.

of about 30–40% when the saturation level is decreased. As the *TR* repetition time was chosen short enough to minimize the acquisition time, the magnetization has not completely returned to equilibrium between two acquisitions and is in a pseudo-equilibrium state. This weighting of the resulting NMR signal is taken into account to a good approximation by measuring the reference intensity, which also undergoes the same variations. The T_2 weighting term produces an error estimated at less than 10%

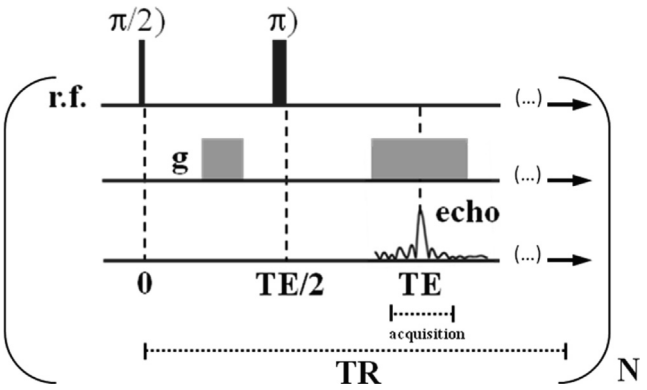

Fig. 2. Temporal diagram of the 1D spin-echo NMR imaging sequence used for the measurement of the moisture profiles.

because the echo time is chosen as short as possible, in any case more than four times shorter than the T_2 relaxation time.

2.2. Materials

The NMR setup described above was used to study the drying behavior of inkjet ink on four different paper substrates. The substrates are printing papers from industrial production, consisting of bleached hardwood pulp and calcium carbonate filler pigment. The papers have been treated differently to modify their water absorption behavior (Fig. 3). The paper with the lowest water absorption rate is a paper treated with AKD – alkyl ketene dimer – a sizing agent acting as water uptake inhibitor ('almost non-absorbing'). For the weakly absorbing paper, a surface layer of pigment particles reduces water absorption ('weakly absorbing'). Water absorption of the moderately absorbing substrate ('moderately absorbing') is lower compared to the strongly absorbing paper ('strongly absorbing') due to a lower surface roughness and surface porosity caused by calendering. Relevant substrate properties are presented in Table 2, a more detailed description of the papers can be found in (Krainer et al., 2019). Grammage was measured according to EN ISO 536, thickness in dry state according to EN ISO 534. Additionally, thickness was also measured of wet samples which had been immersed in deionized water for at least one minute. To determine the porosity, mercury intrusion porosimetry was performed with an Autopore IV 9500 from Micrometics Instruments (Resch et al., 2010). Water absorption rates were measured with an automatic scanning absorptometer (ASA) instrument (Kuijpers et al., 2018). The paper surface thereby is contacted with water via a nozzle moving over the surface at different speeds. Fig. 3 shows the water absorption rate between 30 ms and 130 ms contact time of the nozzle with the substrate. For a more detailed description of the measurement principle, please refer to (Krainer and Hirn, 2018). The ink employed in this study was an ink-jet ink from a large OEM for inkjet printers. These types of ink are mainly composed of water as solvent, together with diethylene-glycol and glycerol as co-solvents, and pigments.

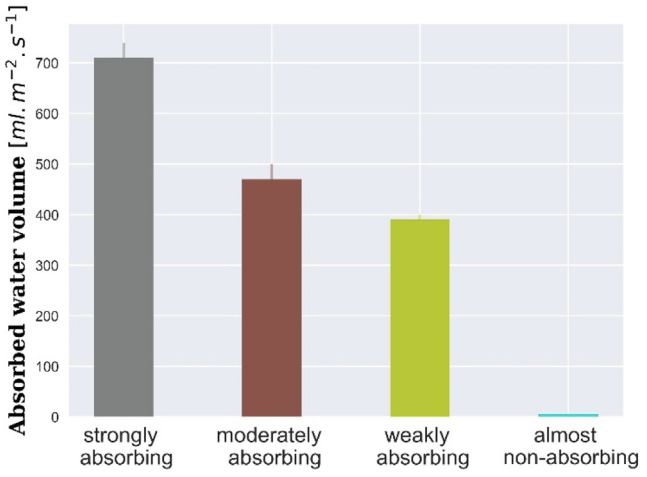

Fig. 3. Water absorption rates of the investigated substrates measured by automatic scanning absorptometer. Error bars are 95% confidence intervals.

2.3. Data processing

The data are collected over a total duration of 64 s, which corresponds to the acquisition of 50 consecutive profiles. As the acquisition starts before the application of the ink in order to capture all the information during the drying process, the time t = 0 does not necessarily correspond to the first recorded profile. Instead, the initial time is subsequently assigned to the profile with the highest intensity. The raw data of the profiles were first filtered using the Wiener function of the scipy.signal library in Python 3.7. A baseline correction was then performed by subtracting the average intensity of the first 50 points. An example of a profile measured on the most absorbent paper is shown in Fig. 4. The signal-to-noise ratio of this measurement, calculated as the ratio of the average intensity of the reference profile and the noise determined on the average of the first points is greater than 40. The black dots correspond to the raw data, the shaded line to the data after filtering.

When needed (e.g., to plot Figs. 7 to 9), profile integration was calculated over a distance of $\sim$ 400 μm (40 points) centered on each profile. The measurements were performed on 7 to 9 samples for each type of paper considered. The error bars in Figs. 6 to 8 represent the standard deviation of each quantity represented, calculated on all the samples tested.

3. Results and discussion

Through thickness moisture profiles based on normalized NMR intensities of the four paper types after different drying times are depicted in Fig. 5. At the beginning of the measurement, a huge moisture gradient over the paper thickness exists for all samples and the profile has a more or less linear shape. Over time, the water distribution within the papers evens out. Knowing the thickness of the samples, one can see that the 129 μm thick strongly absorbing paper had some water already penetrated all through at the beginning of the measurement, while this has taken a few seconds for the 89 μm thick moderately absorbing paper. For the weakly absorbing (92 μm) and the almost non-absorbing (105 μm) paper, on the other hand, the moisture profiles did not extend over the whole thickness of the sheets. This indicates that the water contained in the ink did not penetrate to the back side of the sheets. Fig. 9 includes photographs of the paper backsides after the measurement which confirm that the ink was striking through to the backside for moderately absorbing and strongly absorbing papers, but not so for almost non-absorbing and weakly absorbing papers.

When comparing the evolution of moisture profiles over time, it turns out that the papers' drying behaviors differed considerably. For the moderately absorbing and strongly absorbing paper, the water was redistributed quickly throughout the sheet leading to rather flat profiles after a short amount of time. Also, the NMR intensity decreased fast, indicating quick drying. The almost non-absorbing paper showed hardly any redistribution, as the z-directional moisture profile is not flattening or covering the whole thickness at any time. The intensity of the detected signal however

Table 2
Properties of the paper substrates used in this study.

	Strongly absorbing	Moderately absorbing	Weakly absorbing	Almost non-absorbing
Grammage [g/m^2]	97.20	78.50	79.89	77.20
Thickness (dry) [μm]	129	89	92	105
Thickness (wet) [μm]	154	124	123	125
Porosity [%]	40.3	38.8	23.6	20.6
Water absorption rate [ml·m^{-2}·s^{-1}]	710	470	390	6

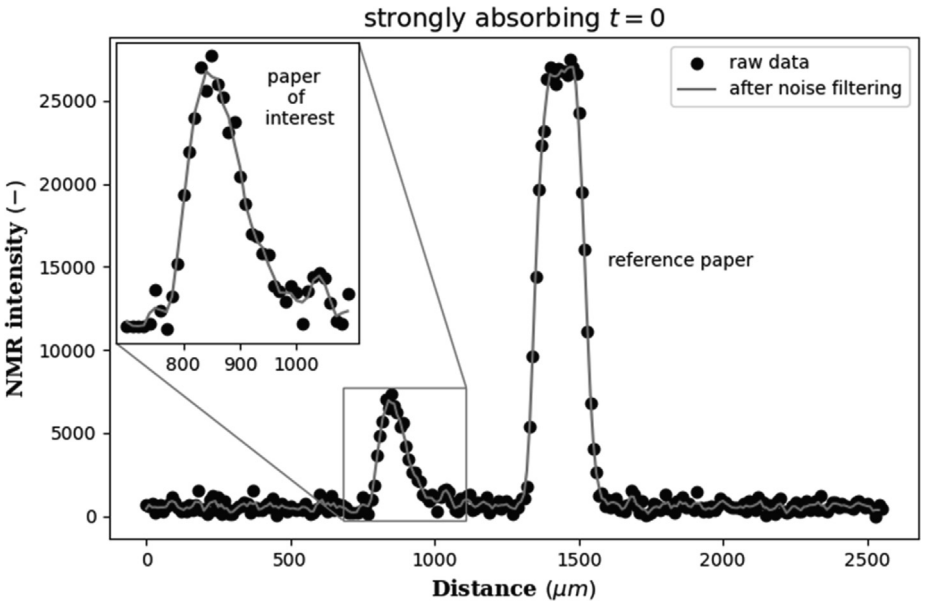

Fig. 4. Example of water profile in a strongly absorbing paper just after ink application (t = 0). The inset shows the shape of the profile in the studied sample, the top side being the left side of the figure. The dots correspond to the raw data, the grey line to the data after application of a filter to reduce the measurement noise (see text). The water profile in the reference sheet is square, showing a uniform distribution.

decreased fast, indicating very fast drying from the top side of the sheet. After only about 10 s the almost non-absorbing paper can essentially be regarded as completely dry. The moisture profiles measured after that exhibit a rather high level of noise. The weakly absorbing paper demonstrated a completely different drying behavior. After a bit less than a minute there was still a considerable moisture gradient over the thickness of the weakly absorbing paper. Seemingly, the water was not redistributed within the sheet and drying was slow. Evaporation from the surface is indicated by the peak of the intensity moving slightly to the right, away from the top side of the paper.

From the z-directional moisture profiles at different points in time, a number of interesting parameters and their evolution over time can be derived. For instance, a measure of the penetration depth can be deduced by evaluating the position within the moisture profile at which the signal intensity has decreased to 50 percent of the maximum intensity (PDHI value: penetration depth at half intensity). Fig. 6 shows the resulting penetration depth over time (blue markers, left axis). Furthermore, the moisture reduction, also shown in Fig. 6 (brown markers, right axis), is defined as the maximum NMR intensity at a given time normalized by the maximum intensity. For moderately absorbing and strongly absorbing paper the maximum penetration depth was reached quickly, before it stayed at a more or less constant level. The water content (signal intensity) decreased in the same time scale. Interestingly, the penetration depth of the constant part is close to the thickness measured on wet samples for both papers. The error bars are rather large for the strongly absorbing paper which is related to noise in the signal. The measurement of the almost non-absorbing paper is strongly affected by noise as well. We know that it is dry already after a few seconds from the profiles in Fig. 5. Penetration depth should not get even close to 100 μm. In this case it would be more meaningful to stop the evaluation after a few seconds. This approach for the determination of the penetration depth works best for the weakly absorbing paper. The graphs in Fig. 6 show that, for the weakly absorbing paper, penetration proceeded to a comparatively small extent and over a rather long period of time, levelling off at less than 50 μm. Less noise is to be expected in this case, as the signal intensity does not decrease to such a low level as for the other papers.

The results discussed so far provide information about temporally resolved moisture distribution in z-direction and liquid penetration depth. However, when describing and interpreting the drying behavior, a local measure of how much liquid was absorbed and needs to be dried would be useful. In order to obtain the information on the liquid saturation, we compared the measurement of the sample to the measurement of the same paper that was fully saturated with liquid. Thus, we can calculate the relative liquid saturation, as the integral of the NMR intensity curve of the sample thickness divided by the integral of the signal of the liquid-saturated reference paper over its thickness. Fig. 7 shows the relative liquid saturation of all samples over time. The moderately absorbing and strongly absorbing paper started with a very high relative saturation of about 15 percent, which is about twice the percentage of the weakly absorbing and three times the percentage of the almost non-absorbing paper. This indicates that the moderately absorbing and strongly absorbing papers took up rather large amounts of liquid, while the almost non-absorbing paper absorbed

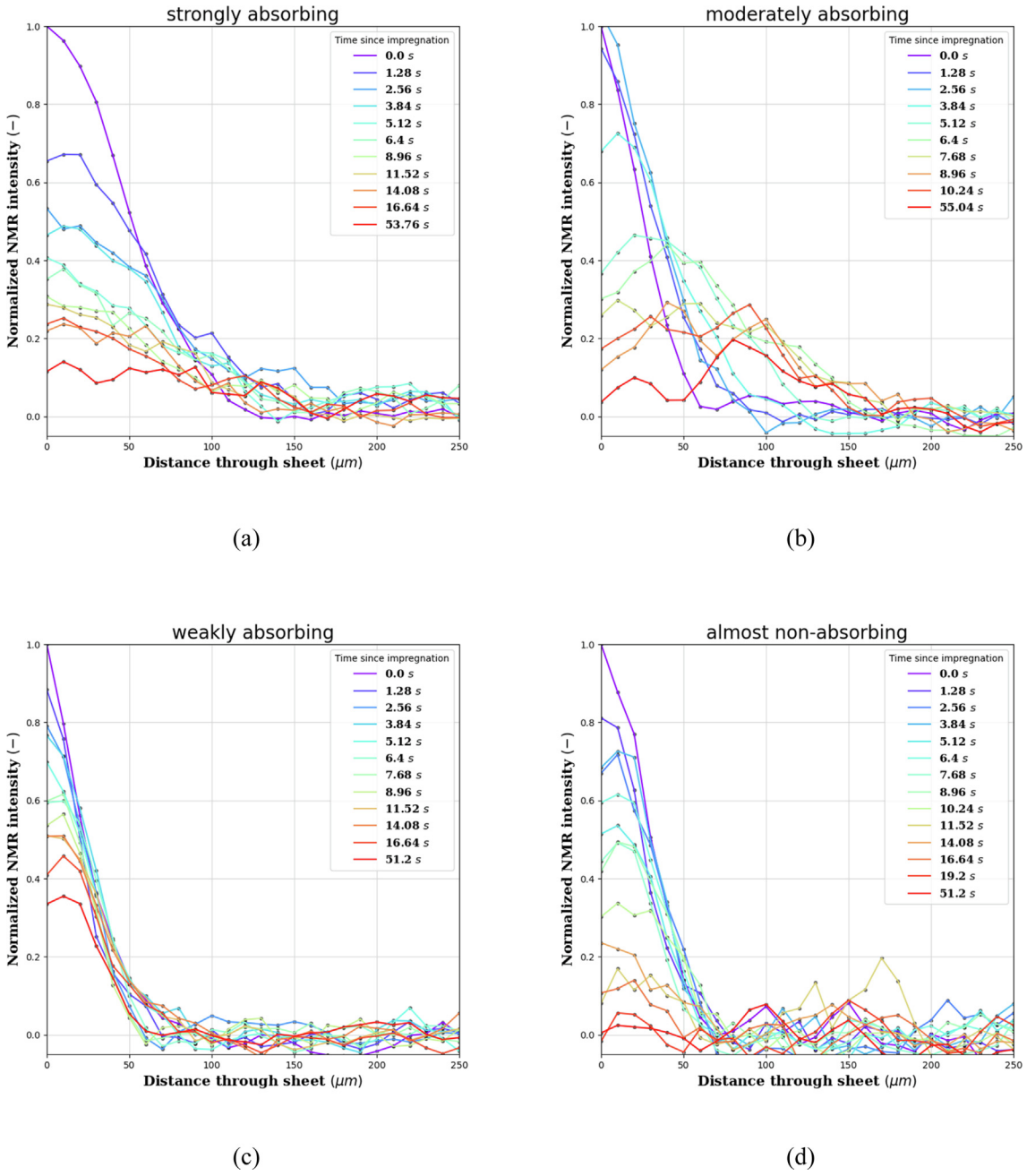

Fig. 5. Through-thickness moisture profiles after different drying times for paper samples (a) strongly absorbing, (b) moderately absorbing, (c) weakly absorbing, and (d) almost non-absorbing.

only a small quantity. Furthermore, the liquid saturation curve of the almost non-absorbing paper also demonstrates that after a bit more than 10 s hardly any liquid was left. This observation not only provides further evidence for the fast drying of the almost non-absorbing paper, but also delivers an explanation for it, as it shows that a much lower liquid amount was present already at the start.

The relative liquid saturation values agree well with the water absorption measurements presented in Fig. 3. The most strongly absorbing paper also exhibits the highest liquid saturation values while the almost non-absorbing paper also reaches only low levels of liquid saturation.

Interestingly, the liquid saturation difference between moderately absorbing and strongly absorbing paper on the one hand and weakly absorbing paper on the other hand disappears after the first 10 to 15 s of drying. To get a better understanding of this effect, it is useful to introduce another parameter to study the kinetics of drying. Fig. 8 shows time dependent curves of the integrated NMR signal normalized to the first measurement. By evaluating the change of the NMR intensity throughout the whole profile over time, the drying kinetics can be observed, as it reflects how the water content in the sample diminishes. The curve of the weakly absorbing paper is less steep than the other papers' curves indicating slower drying. The slower drying could be caused by the surface pigment layer of the weakly absorbing paper that is probably impeding water transport to the surface. The moisture profiles after 16 and more seconds (Fig. 5), which show a higher water amount within the sheet than at the surface, support this hypothesis. The other three papers dried equally fast at the beginning of the measurement. After a few seconds, however, the drying rate

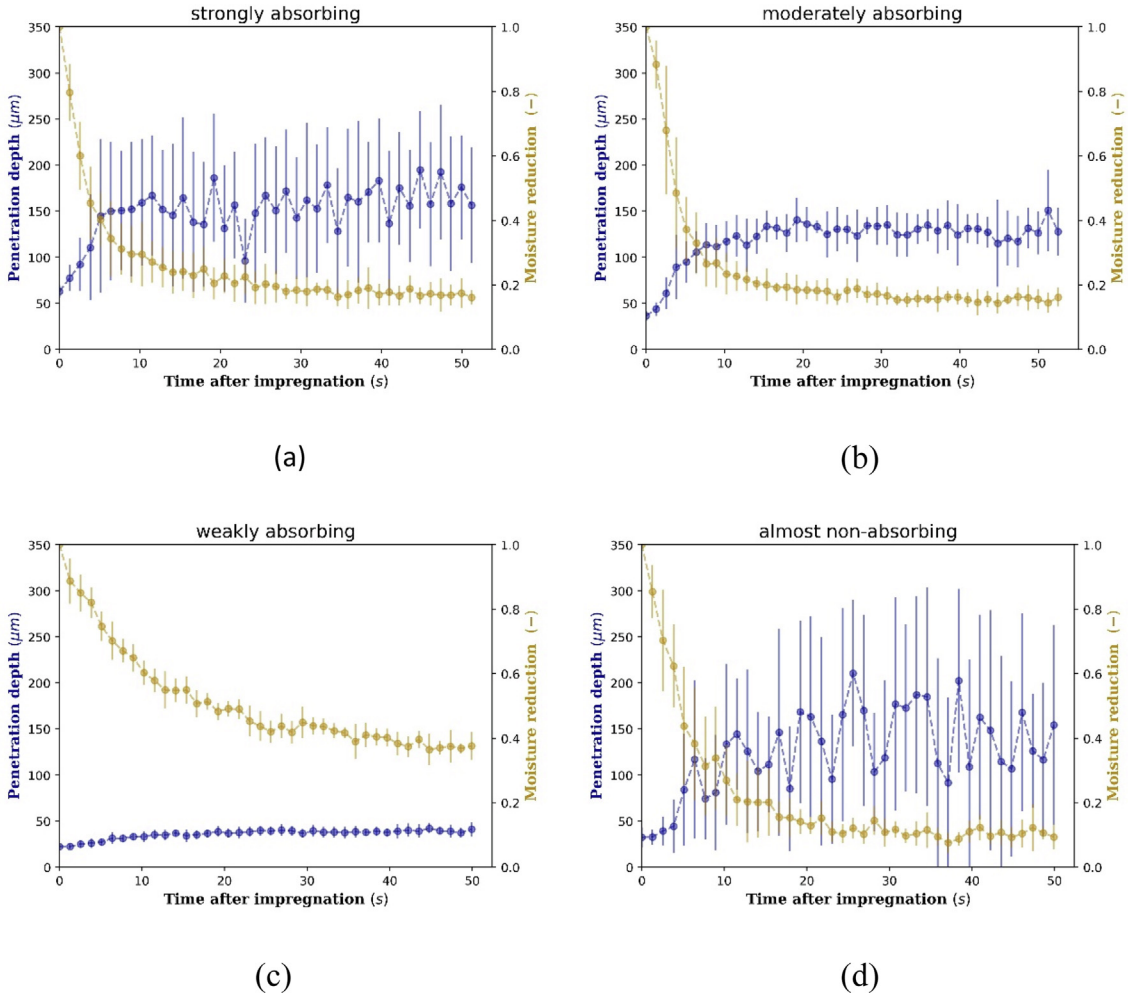

Fig. 6. Penetration depth over time (blue markers, left axis) and moisture reduction (brown markers, right axis) for the papers (a) strongly absorbing, (b) moderately absorbing, (c) weakly absorbing, and (d) almost non-absorbing. Penetration depth was defined as the PDHI value of the distribution, moisture reduction as the normalized maximum signal.

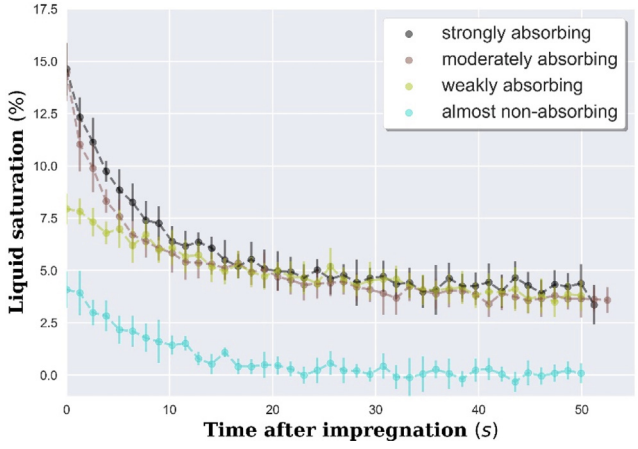

Fig. 7. Relative liquid saturation of samples over time. Relative liquid saturation was calculated as the integral of the signal in the sample divided by the integral of the signal of the saturated reference paper.

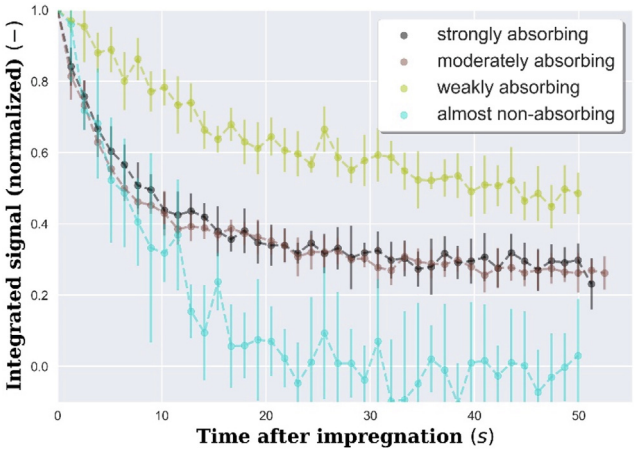

Fig. 8. Drying kinetics of the different substrates. Evolution of integrated NMR signal over time, normalized to integral of first profile (t = 0 s). The change of the normalized, integrated signal provides information about the drying speed.

of the strongly absorbing and moderately absorbing paper decreased and the curve leveled off, while the almost non-absorbing paper curve decreased to close to zero within about 15 to 20 s. A value of zero indicates that no significant amounts of water are present anymore, which again shows that the almost non-absorbing paper was completely dry after a short amount of time. The decrease in the drying rate of moderately absorbing and strongly absorbing paper can be explained by the measure-

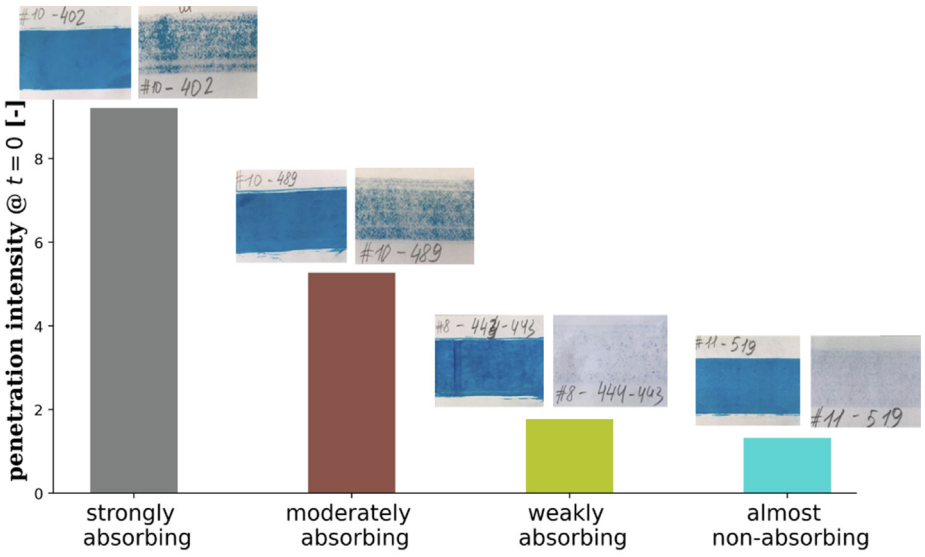

(a)

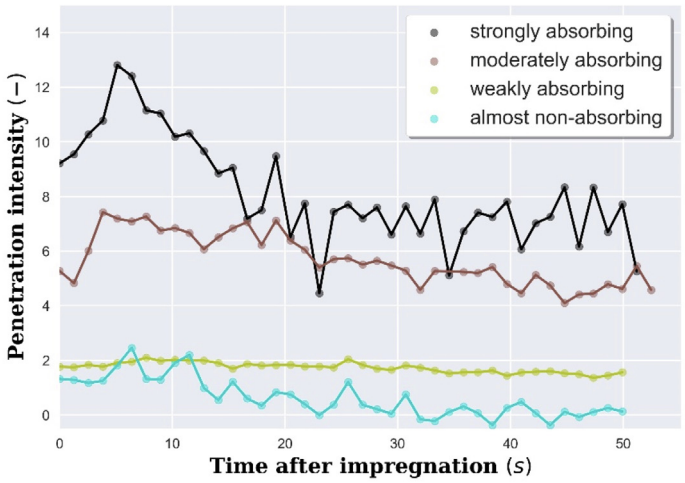

(b)

Fig. 9. Penetration intensity: (a) at the beginning of the measurement (t = 0 s); (b) evolution over time. Penetration intensity is calculated as penetration depth multiplied with relative liquid saturation.

ment setup. The space within the measurement chamber is very limited and both papers took up a large amount of liquid. Thus, it is probable that the surrounding air was more and more saturated with moisture which in turn led to the decrease in drying rate. Furthermore, it is possible that the fiber surface hydrophobization of the almost non-absorbing paper with AKD prevented deeper penetration of the liquid into the fibers and the bulk of the sheet, which makes drying easier.

When it comes to drying effort, both liquid amount and penetration depth of the liquid into the bulk of the sheet will play a role, as the liquid has to be transported to the surface and evaporated for drying. A combined parameter employing liquid penetration depth and liquid saturation could reflect their combined impact on the required drying intensity. We call this parameter penetration intensity and calculate it as penetration depth multiplied by liquid saturation. Fig. 9 shows penetration intensity (a) at the beginning of the measurement and (b) its development over time. While the moderately absorbing and strongly absorbing paper exhibited only minor differences in drying kinetics and liquid saturation, they differed significantly more in terms of penetration intensity. The strongly absorbing paper thereby clearly displayed the highest penetration intensity. This is in line with the strongly absorbing paper absorbing much greater water amounts than the moderately absorbing paper in the ASA measurements (Fig. 3). In addition, the almost non-absorbing paper exhibiting the lowest penetration intensity is consistent with the ASA measurements as well. Furthermore, penetration intensity values also match the visual impression of the sample backsides after the measurements. Penetration intensity over time decreases more slowly than liquid saturation. For moderately absorbing and strongly absorbing paper it even increased initially. That is caused by the liquid still penetrating or diffusing further into the substrate. As penetration depth is not declining over time (compare Fig. 6), penetration intensity can move towards zero only if liquid saturation does so too. In that

way, penetration intensity over time shows, that the almost non-absorbing paper is the only paper that was completely dried within the measurement time. Moreover, the combination of penetration depth and liquid saturation in one parameter also relativizes the high level of noise in the penetration depth curve of the almost non-absorbing paper. All in all, it might be a useful parameter to estimate how intensively a substrate has been penetrated by the liquid and how much effort will be necessary for drying it. A precondition for a direct comparison between papers, however, is that they absorb similar liquid amounts in the fully saturated state, as this affects relative liquid saturation.

4. Conclusions

We have introduced an NMR based setup for comprehensive *z*-directional analysis of liquid distribution and migration in thin sheets. The 1D NMR profiling method presented in this work can be used for sheets of about 100 μm thickness and liquid absorption, migration and drying in *z*-direction of the sheets can be observed. This can be achieved thanks to the good temporal resolution of 1.3 s and the high spatial resolution of about 10 μm in thickness direction of the sheets.

A key aspect of our method is simultaneous measurement of a liquid saturated reference sheet during each measurement. Having reference NMR intensities for a liquid saturated sheet it is possible to calculate local liquid saturation and the absolute amount of liquid present in the sheet. Based on this the kinetics of liquid absorption and drying can be analyzed more effectively, particularly when the liquid absorption of different substrates is not known a priori.

We applied this method to observe the drying of water-based inkjet ink on four papers with differing water absorption behaviors. Results show differences in *z*-directional liquid distribution, penetration depth, and drying kinetics over time. It could be shown that penetration depth and liquid saturation were lower for the AKD sized, almost non-absorbing paper which resulted in faster drying compared to the other papers studied. We believe that this method is a suitable tool to quantify absorption, migration and drying processes, and thus supports a better understanding of moisture distribution- and transport processes in thin sheets.

CRediT authorship contribution statement

Jean-Christophe Perrin: Conceptualization, Methodology, Data curation, Validation, Formal analysis, Investigation, Writing – original draft, Writing – review & editing, Supervision, Visualization. **Carina Waldner:** Writing – original draft, Writing – review & editing, Visualization. **Julie Bossu:** Conceptualization, Methodology, Investigation. **Aninda Chatterjee:** Software, Formal analysis, Visualization. **Ulrich Hirn:** Methodology, Conceptualization, Writing – original draft, Writing – review & editing, Supervision, Project administration, Funding acquisition.

Declaration of Competing Interest

The authors declare that they have no known competing financial interests or personal relationships that could have appeared to influence the work reported in this paper.

Acknowledgements

The financial support by the Austrian Federal Ministry for Digital and Economic Affairs and the National Foundation for Research Technology and Development is gratefully acknowledged. We also thank our industrial partners Mondi, Canon Production Printing, Kelheim Fibres, and SIG Combibloc for their financial support.

References

Banerjee, D., von Spiegel, W., Thomson, M.D., Schabel, S., Roskos, H.G., 2008. Diagnosing water content in paper by terahertz radiation. Opt. Express 16 (12), 9060.
Batchelor, W.J., Wu, Z., Johnston, R.E., 2004. Measurement of z-direction moisture transport and shrinkage in the drying of paper. Appita J. 57, 107–111.
Bencsik, M., Adriaensen, H., Brewer, S.A., McHale, G., 2008. Quantitative NMR monitoring of liquid ingress into repellent heterogeneous layered fabrics. J. Magn. Reson. 193 (1), 32–36. https://doi.org/10.1016/j.jmr.2008.04.003.
Bennett, G., Gorce, J.-P., Keddie, J.L., McDonald, P.J., Berglind, H., 2003. Magnetic resonance profiling studies of the drying of film-forming aqueous dispersions and glue layers. Magn. Reson. Imaging 21 (3-4), 235–241. https://doi.org/10.1016/S0730-725X(03)00130-9.
Ciampi, E., McDonald, P.J., 2003. Skin formation and water distribution in semicrystalline polymer layers cast from solution: A magnetic resonance imaging study. Macromolecules 36, 8398–8405. https://doi.org/10.1021/ma034951j.
Erich, S.J.F., Laven, J., Pel, L., Huinink, H.P., Kopinga, K., 2006. NMR depth profiling of drying alkyd coatings with different catalysts. Prog. Org. Coatings 55 (2), 105–111. https://doi.org/10.1016/j.porgcoat.2005.08.009.
Erich, S.J.F., Laven, J., Pel, L., Huinink, H.P., Kopinga, K., 2005. Dynamics of cross linking fronts in alkyd coatings. Appl. Phys. Lett. 86, 1–3. https://doi.org/10.1063/1.1886913.
Forughi, A.F., Green, S., Stoeber, B., 2019. Effect of dryer fabric structure on the performance of contact paper drying. Dry. Technol. 37 (7), 854–863. https://doi.org/10.1080/07373937.2018.1469141.
Forughi, A.F., Green, S.I., Stoeber, B., 2016. Optical transparency of paper as a function of moisture content with applications to moisture measurement. Rev. Sci. Instrum. 87 (2), 023706. https://doi.org/10.1063/1.4942251.
Gane, P.A.C., Koivunen, K., 2010. Relating liquid location as a function of contact time within a porous coating structure to optical reflectance. Transp. Porous Media 84 (3), 587–603. https://doi.org/10.1007/s11242-009-9523-x.
Harding, S.G., Wessman, D., Stenström, S., Kenne, L., 2001. Water transport during the drying of cardboard studied by NMR imaging and diffusion techniques. Chem. Eng. Sci. 56 (18), 5269–5281. https://doi.org/10.1016/S0009-2509(01)00197-X.
Hellgren, A.-C., Wallin, M., Weissenborn, P.K., McDonald, P.J., Glover, P.M., Keddie, J. L., 2001. New techniques for determining the extent of crosslinking in coatings. Prog. Org. Coatings 43 (1-3), 85–98. https://doi.org/10.1016/S0300-9440(01)00215-6.
Hughes, P.D.M., McDonald, P.J., Rhodes, N.P., Rockliffe, J.W., Smith, E.G., Wills, J., 1996. A stray field magnetic resonance imaging study of the drying of sodium silicate films. J. Colloid Interface Sci. 177 (1), 208–213. https://doi.org/10.1006/jcis.1996.0022.
Kajihara, Y., Tamura, Y., Matsuzaka, K., Kadoya, S., Kimura, F., 2017. Measuring the moisture content of pulp injection molded products with terahertz waves. Int. J. Autom. Technol. 11 (5), 766–771.
Katugampola, P., Loffler, S., Batchelor, W., Johnston, R.E., 2006. Measurement of water penetration and swelling in a multilayered sheet. Appita Annu. Conf. 2006, 199–204.
Keränen, J.T., Paaso, J., Timofeev, O., Kiiskinen, H., 2009. Moisture and temperature measurement of paper in the thickness direction. Appita J. 62, 308–313.
Ketelaars, A.A.J., Pel, L., Coumans, W.J., Kerkhof, P.J.A.M., 1995. Drying kinetics: A comparison of diffusion coefficients from moisture concentration profiles and drying curves. Chem. Eng. Sci. 50, 1187–1191. https://doi.org/10.1016/0009-2509(94)00494-C.
Klein, M., Perrin, J.-C., Leclerc, S., Guendouz, L., Dillet, J., Lottin, O., 2013. Spatially and temporally resolved measurement of water distribution in nafion using NMR imaging. ECS Trans. 58 (1), 283–289. https://doi.org/10.1149/05801.0283ecst.
Koivunen, K., Gane, P.A.C., 2012a. Impact of oil-binder interaction on pore structure in paper coatings as studied by internal reflectance Part 1: Implications of pore volume loss for print drying. Nord. Pulp Pap. Res. J. 27, 757–764. https://doi.org/10.3183/NPPRJ-2012-27-04-p757-764.
Koivunen, K., Gane, P.A.C., 2012b. Impact of oil-binder interaction on pore structure in paper coatings as studied by internal reflectance. Part 2: Relation to structural expansion. Nord. Pulp Pap. Res. J. 27, 765–773. https://doi.org/10.3183/NPPRJ-2012-27-04-p765-773.
Krainer, S., Hirn, U., 2018. Short timescale wetting and penetration on porous sheets measured with ultrasound, direct absorption and contact angle. RSC Adv. 8, 12861–12869. https://doi.org/10.1039/c8ra01434e.
Krainer, S., Smit, C., Hirn, U., 2019. The effect of viscosity and surface tension on inkjet printed picoliter dots. RSC Adv. 9 (54), 31708–31719.
Kuijpers, C.J., van Stiphout, T.A.P., Huinink, H.P., Tomozeiu, N., Erich, S.J.F., Adan, O.C. G., 2018. Quantitative measurements of capillary absorption in thin porous media by the Automatic Scanning Absorptometer. Chem. Eng. Sci. 178, 70–81. https://doi.org/10.1016/j.ces.2017.12.024.
Leisen, J., Hojjatie, B., Coffin, D.W., Lavrykov, S.A., Ramarao, B.V., Beckham, H.W., 2002. Through-plane diffusion of moisture in paper detected by magnetic

resonance imaging. Ind. Eng. Chem. Res. 41 (25), 6555–6565. https://doi.org/10.1021/ie0204686.
MacMillan, M.B., Schneider, M.H., Sharp, A.R., Balcom, B.J., 2002. Magnetic resonance imaging of water concentration in low moisture content wood. Wood Fiber Sci. 34, 276–286.
Neacsu, V., Leisen, J., Beckham, H.W., Advani, S.G., 2007. Use of magnetic resonance imaging to visualize impregnation across aligned cylinders due to capillary forces. Exp. Fluids 42 (3), 425–440. https://doi.org/10.1007/s00348-007-0251-0.
Nicasy, R., Huinink, H.P., Erich, S.J.F., Adan, O.C.G., 2021. High-speed NMR imaging of capillary action in thin nontransparent porous media. Phys. Rev. E 104, 2–6. https://doi.org/10.1103/PhysRevE.104.L043101.
Nilsson, L., Mansson, S., Stenstrom, S., 1996. Measuring moisture gradients in cellulose fibre networks: An application of the magnetic resonance imaging method. J. Pulp Pap. Sci., 22
Nizovtsev, M.I., Stankus, S.V., Sterlyagov, A.N., Terekhov, V.I., Khairulin, R.A., 2008. Determination of moisture diffusivity in porous materials using gamma-method. Int. J. Heat Mass Transf. 51 (17-18), 4161–4167. https://doi.org/10.1016/j.ijheatmasstransfer.2008.01.013.
Pel, L., Ketelaars, A.A.J., Adan, O.C.G., Van Well, A.A., 1993. Determination of moisture diffusivity in porous media using scanning neutron radiography. Int. J. Heat Mass Transf. 36 (5), 1261–1267. https://doi.org/10.1016/S0017-9310(05)80095-X.
Resch, P., Bauer, W., Hirn, U., 2010. Calendering effects on coating pore structure and ink setting behavior. Tappi J. 9, 27–35. https://doi.org/10.32964/tj9.1.27.
Rosenkilde, A., Glover, P., 2002. High resolution measurement of the surface layer moisture content during drying of wood using a novel magnetic resonance imaging technique. Holzforschung 56, 312–317. https://doi.org/10.1515/HF.2002.050.
Salamanca, J.M., Ciampi, E., Faux, D.A., Glover, P.M., McDonald, P.J., Routh, A.F., Peters, A.C.I.A., Satguru, R., Keddie, J.L., 2001. Lateral drying in thick films of waterborne colloidal particles. Langmuir 17 (11), 3202–3207. https://doi.org/10.1021/la001590h.
Tåg, C.-M., Juuti, M., Koivunen, K., Gane, P.A.C., 2010a. Dynamic water transport in a pigmented porous coating medium: Novel study of droplet absorption and evaporation by Near-infrared spectroscopy. Ind. Eng. Chem. Res. 49 (9), 4181–4189. https://doi.org/10.1021/ie1000289.
Tåg, C.-M., Toiviainen, M., Juuti, M., Gane, P.A.C., 2010b. Dynamic analysis of temporal moisture profiles in heatset printing studied with near-infrared spectroscopy. Meas. Sci. Technol. 21 (10), 105602. https://doi.org/10.1088/0957-0233/21/10/105602.
Uesaka, T., 2002. In: Mark, R.E., Habeger, C.C., Borch, J., Lyne, M.B. (Eds.), Handbook of Physical Testing of Paper -, 1. CRC Press, Boca Raton, FL, pp. 115–171 https://doi.org/10.1201/9781482290103.
Varga, K., Hameed, F., Zawisky, M., Schuster, K.C., 2009. Distribution of water in filling fibres visualised by neutron radiography. Lenzinger Berichte 87, 124–134.
Voogt, B., Huinink, H., Erich, B., Scheerder, J., Venema, P., Adan, O., 2018. Water mobility during drying of hard and soft type latex: Systematic GARField 1H NMR relaxometry studies. Prog. Org. Coatings 123, 111–119. https://doi.org/10.1016/j.porgcoat.2018.06.011.
Wallin, M., Glover, P.M., Hellgren, A.-C., Keddie, J.L., McDonald, P.J., 2000. Depth profiles of polymer mobility during the film formation of a latex dispersion undergoing photoinitiated cross-linking. Macromolecules 33 (22), 8443–8452. https://doi.org/10.1021/ma000787d.
Weder, M., Brühwiler, P.A., Laib, A., 2006. X-ray tomography measurements of the moisture distribution in multilayered clothing systems. Text. Res. J. 76 (1), 18–26. https://doi.org/10.1177/0040517506053910.